Generation of ultrashort coherent radiation based on a laser plasma accelerator

Tao Liu,[a] Chao Feng,[a]* Dao Xiang,[b] Jiansheng Liu[c] and Dong Wang[a]

[a]Shanghai Institute of Applied Physics, Chinese Academy of Sciences, Shanghai 201800, People's Republic of China, [b]Department of Physics and Astronomy, Key Laboratory for Laser Plasmas, Shanghai Jiao Tong University, Shanghai 200240, People's Republic of China, and [c]Shanghai Institute of Optics and Fine Mechanics, Chinese Academy of Sciences, Shanghai 201800, People's Republic of China. *Correspondence e-mail: fengchao@sinap.ac.cn

A laser plasma accelerator (LPA) has the potential to realize compact free-electron laser (FEL) radiation at the regular laboratory scale. However, large initial angular divergence and energy spread dramatically hinder ways to transport the beam and realize FEL radiation. Although methods have been proposed to solve these problems, the relatively large jitter, including transverse position jitter and energy jitter, still limits the advance of these experiments. In this paper a simple method to realize coherent harmonic generation based on a LPA beam is proposed. The scheme is very compact, adopting a high-power laser split from the driver laser, a short modulator and a short radiator which has a great tolerance to these typical types of jitter. Numerical simulations indicate that coherent third-harmonic radiation with gigawatt-level power and single spike spectra can be obtained, verifying the feasibility of the scheme and indicating the capability to generate ultrashort fully coherent radiation.

1. Introduction

Free-electron lasers (FELs) (Huang & Kim, 2007) based on the conventional radio-frequency (RF) linear accelerator represent a revolution in light source development, opening up new frontiers of ultrafast and ultrasmall science at atomic length scales (Bostedt et al., 2016; Young et al., 2010; Chapman et al., 2011). FELs have been in operation for users with the great success of several operational facilities around the world, such as LCLS at SLAC, FERMI at Eletta, FLASH at DESY and SACLA at SPring-8 (Emma et al., 2010; Allaria et al., 2012; Ackermann et al., 2007; Ishikawa et al., 2012). However, these facilities based on RF technology are usually very large, up to several kilometres, which significantly increases the expense and hinders the way for the wider application of the FEL. It is therefore desirable to dramatically reduce the size and cost of the X-ray FEL to the university-laboratory scale.

Compact FELs driven by a laser plasma accelerator (LPA) have the potential to achieve such a goal (Schroeder et al., 2006; Grüner et al., 2007; Nakajima, 2008; Fuchs et al., 2009). Recently, the LPA has successfully generated an electron beam with an energy of a few GeV within a centimetre scale of the accelerating distance (Tajima & Dawson, 1979; Esarey et al., 2009; Wang et al., 2013; Kim et al., 2013; Leemans et al., 2014; Liu et al., 2011; Li et al., 2015; Wang et al., 2016). Typical properties of the LPA beam are a peak current of up to tens of kiloamps, a pulse duration of the order of several femtoseconds and a normalized transverse emittance below 1 mm mrad (Liu et al., 2011). The major problems with the LPA beam for FEL generation are large initial divergence (up to 1 mrad) and large energy spread ($\sim$1%) which drastically

Plasma gas / Seed laser (266nm) / Harmonic generation / ~100TW laser / Quadrupole triplet / Modulator / Radiator / Vacuum chamber
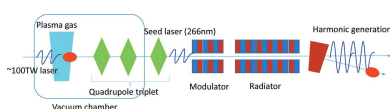
increase the difficulty of transporting the LPA beam from the accelerator to the undulators and cause degradation of the FEL radiation gain.

In the FEL community, some specific methods based on transverse gradient undulators (TGUs) and decompression have been proposed to minimize the energy spread effect leading to a substantial improvement in FEL gain and radiation power (Huang *et al.*, 2012; Schroeder *et al.*, 2013; Maier *et al.*, 2012; Loulergue *et al.*, 2015; Widmann *et al.*, 2013, 2014; Liu *et al.*, 2016, 2017). However, due to the relatively large energy jitter and transverse jitter experimentally, it is difficult to transport the LPA beam in the beamline, as well as carrying out the next step, *i.e.* generating FEL radiation.

An alternative method based on the coherent harmonic generation (CHG) technique (Yu, 1991; Yu *et al.*, 2000; Girard *et al.*, 1984) can be considered, which has been widely used in storage rings and high-gain FELs in the UV–VUV wavelength range (Yu *et al.*, 2000; Labat *et al.*, 2007; De Ninno *et al.*, 2008; Xiang & Wan, 2010; Feng *et al.*, 2015). According to FEL theory, a pre-bunched electron beam with a high bunching factor could directly generate coherent radiation at wavelength λ/n within a very short undulator, where n is the harmonic number. A standard CHG scheme generally consists of a modulator and a radiator with a chicane in between. An external seed laser is used to interact with the electron beam in the short modulator and induces a sinusoidal energy modulation along the longitudinal beam position. Such an energy modulation will be converted into a longitudinal density modulation after the beam passes through the small chicane, *i.e.* the so-called pre-bunched beam. Owing to the Fourier harmonic components of the pre-bunched beam, fully coherent radiation could be rapidly produced at the high harmonics of the seed laser in the short radiator. Generally, the output radiation peak power of CHG is given by (Yu, 1991)

$$P_{\mathrm{CHG}} = \frac{Z_0 I_{\mathrm{p}}^2 K_0^2 b_n^2 [JJ]^2 L_{\mathrm{u}}^2}{32\pi \Sigma_{\mathrm{A}} \gamma^2}, \qquad (1)$$

where $Z_0 = 377\ \Omega$ is the impedance of free space, K_0 is the undulator parameter with the field-coupling factor $[JJ] = [J_0(\xi) - J_1(\xi)]$, where $\xi = K_0^2/(4 + 2K_0^2)$, L_{u} is the radiator length, and γ, I_{p}, Σ_{A} and b_n are the relative energy, the peak current, the transverse area and the nth bunching factor of the electron beam, respectively. Accordingly, the peak power is mostly determined by the peak current, the bunching factor and the transverse beam size of the electron beam and is almost independent of the electron beam energy spread. For an electron beam with an energy spread σ_δ much smaller than the FEL Pierce parameter ρ, the emission process usually includes an early CHG process and a later FEL exponential gain process. For an electron beam from the LPA, $\sigma_\delta \gg \rho$, and it is difficult to obtain the exponential gain. However, the radiation from CHG can still be very intense since I_{p} is very high for an electron beam from an LPA.

In this paper we propose a novel and simple scheme for the generation of an ultrashort fully coherent radiation pulse with an LPA based on the CHG technique. This proposal makes full use of an ultrahigh-power seed laser which is split from the initial driver laser of the LPA and can effectively induce a large modulation with respect to the large energy spread. Adoption of the driver laser splitting gives the huge advantage that the electron beam keeps a natural time synchronization with the split seed laser, effectively avoiding time jitter and improving the efficiency of the experiment. It is also found that such a large energy modulation can be rapidly converted into a density modulation by the inherent dispersion of the undulator itself. Hence, the proposed scheme does not require a chicane in-between, and is therefore quite simple and compact, enabling beam transport and a compact FEL. The proposed scheme is used for the generation of ultrashort VUV radiation in the LPA. In Section 2 we will introduce the general scheme layout, which includes beam transport and FEL radiation. Section 3 presents numerical simulations. We track an ideal LPA beam through this beamline, present the radiation results and simultaneously analyze the effects of beam jitter in Section 4. A conclusion is drawn in Section 5.

2. Design study of the CHG-FEL based on the LPA

For an LPA beam, it is very challenging to accomplish beam transport due to the large initial divergence, energy spread and various types of jitter. The simplest idea is keeping the FEL setup close to the plasma jet without any beam optics. Thus the total length of the beam transport can be less than 1 m. Assuming a beam with an initial size of 2 μm and divergence 0.3 mrad, the beam size will expand to 300 μm at the exit of the radiator, which enables CHG radiation. Due to limitations of some practical issues, a simple beamline including several quadrupoles is required. The layout of the proposed scheme is shown in Fig. 1. The LPA beam is generated from the plasma gas driven by a powerful laser. The consequent triplet consisting of three quadrupoles is used to pre-focus the beam.

From the powerful driver laser of the LPA with 100 TW power, a small portion with a power of several TW is split off to be a seed laser. The seed laser will be injected into the modulator with a small incidence angle close to the plasma cell to interact with the pre-focused electron beam. The modulator
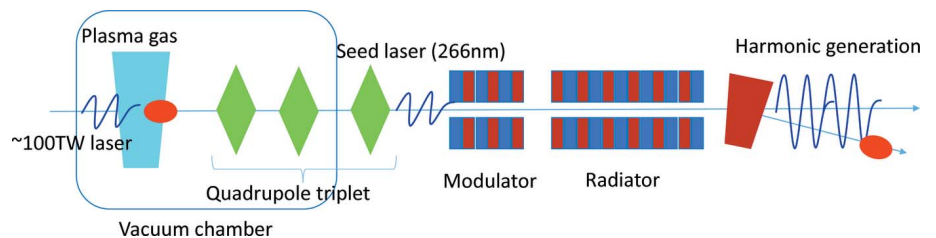

Figure 1
Layout of the proposed CHG-FEL scheme based on an LPA facility.

Table 1
Main parameters of the LPA beam.

Parameter	Symbol	Value	Unit
Relative energy	γ_0	800	mc^2
Emittance	ε_n	0.5	μm
Beam size	σ_{x_0, y_0}	2	μm
Divergence	$\sigma_{x_0', y_0'}$	300	μrad
Peak current	I_0	8	kA
Bunch length (r.m.s.)	σ_{s_0}	1	μm
Energy spread	σ_{δ_0}	1%	–

is very short, since the powerful laser produces enormous energy modulation and the dispersion of the modulator is large enough to convert the energy modulation into a density modulation. The microbunched beam is then sent into a very short radiator tuned to a target harmonic frequency of the seed laser to generate coherent radiation at shorter wavelength.

The main parameters of the LPA beam are listed in Table 1 (Liu *et al.*, 2011; Wang *et al.*, 2016). We firstly optimize the beam Twiss parameters from the plasma jet to the modulator using quadrupoles. These three quadrupoles are aligned quite close to the plasma jet with high magnetic field gradient up to 250 T m^{-1} using the permanent magnetic quadrupole technique (Ghaith *et al.*, 2017). Since the total length of the FEL section is less than 1 m, we consider optimizing the beam waist in the middle of the FEL section, instead of matching a FODO cell in the section. Fig. 2 shows the evolution of the beam sizes with respect to the position z. From 0.7 m to 2 m, both of the beam sizes in the x and y direction are relatively small, where the beam waist is located at 1.3 m, and here the modulator and the radiator would be aligned. The average beam sizes can be easily controlled below 100 μm from the modulator to the radiator due to the very compact layout.

Next let us consider the energy modulation and density modulation processes for the proposed scheme. The energy change of the electron beam along the beam modulated by the seed laser is given by (Hemsing *et al.*, 2014)
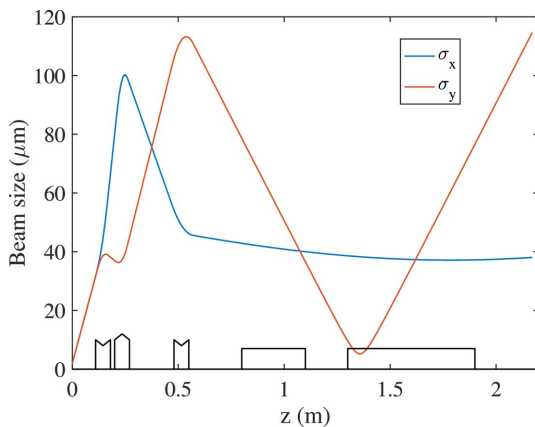

Figure 2
The optimized evolutions of the beam sizes along the beamline. The quadrupole triplet is located within the first 0.6 m, and the 0.3 m modulator and the 0.6 m radiator are aligned from 0.7 m to 2 m.

$$\Delta\gamma(s) = \left(\frac{P_1}{P_0}\right)^{1/2} \frac{2K[JJ]L_u}{\gamma w_0} \cos(k_1 s), \qquad (2)$$

where P_1, w_0 and k_1 are the laser beam power, waist and wavenumber, respectively. $K[JJ]$ and L_u are the modulator undulator strength and length, $P_0 = I_A mc^2/e \simeq 8.7$ GW with an Alfvén current of $I_A \simeq 17$ kA. In order to achieve a good overlap between the electron beam and the laser beam, the laser beam waist w_0 should be larger than the electron beam size of hundreds of micrometres. The modulator length L_u is less than 0.5 m and the modified undulator parameter $K[JJ]$ is basically less than 5. As we know, the required energy modulation amplitude should be several times the energy spread of the LPA beam. Hence, the modulation amplitude $\Delta\gamma$ is very large for the LPA beam, and the seed laser power P_1 should be in the range from hundreds of gigawatts to several terawatts. For a conventional laser, the power is usually at the megawatts level which is several orders of magnitude lower than the laser power required. In our case, we consider that the seed laser is split from the 100 TW driver laser. In order to generate coherent radiation in the VUV or EUV wavelength range, the split laser pulse is chosen as the third-harmonic generation of the driver laser with at least a power of hundreds of gigawatts.

Analyzing the modulator, we have to consider the energy modulation and density modulation simultaneously. The bunching factor of the CHG scheme is given by (Yu, 1991)

$$b_n = J_n(nAB) \exp\left(-\frac{1}{2}n^2B^2\right), \qquad (3)$$

with laser-induced energy modulation amplitude $A = \Delta\gamma/\sigma_\gamma$ and chicane-induced dispersion strength $B = R_{56}k_1\sigma_\gamma/\gamma$. Differing from the chicane-induced dispersion downstream of the energy modulation, the modulator-induced dispersion and the laser-induced energy modulation keep occurring simultaneously within the modulator. Based on the quasi-linear coupled modulation process for this case, the modulator-induced dispersion strength is treated as half of the chicane-induced one. Hence, we can approximate the dispersion strength as $B = (1/2)R_{56}k_1\sigma_\gamma/\gamma$, where $R_{56} = 2\lambda_1/\lambda_u z$ is the longitudinal dispersion of the undulator. Consequently, the dispersion strength B can be briefly written as: $B = \sigma_\delta k_u z$.

Assuming a 6 cm period length undulator, it is calculable that $B \simeq z = 0.06N$ where N is the undulator period number for the beam with an energy spread of 1%. As shown in Fig. 3, the bunching factors as a function of the harmonic numbers are calculated. We consider energy modulation amplitudes $A = 5$ and $A = 10$, and dispersion B in the range 0.05–0.3 determined by the undulator length. The bunching factors for $A = 10$ are larger than those for $A = 5$, particularly for the higher harmonics. The maximums appear at $B \simeq 0.25$ for $A = 5$ and at $B \simeq 0.15$ for $A = 10$. If $B = 0.3$, we can obtain the third-harmonic maximum bunching factor $b_3 \simeq 0.3$. Accordingly, a five-period modulator ($N = 5$, $L_m = 0.3$ m) is long enough for the energy and density modulation process.

Propagating through the modulator, the beam has been microbunched, and will be directly injected into the radiator
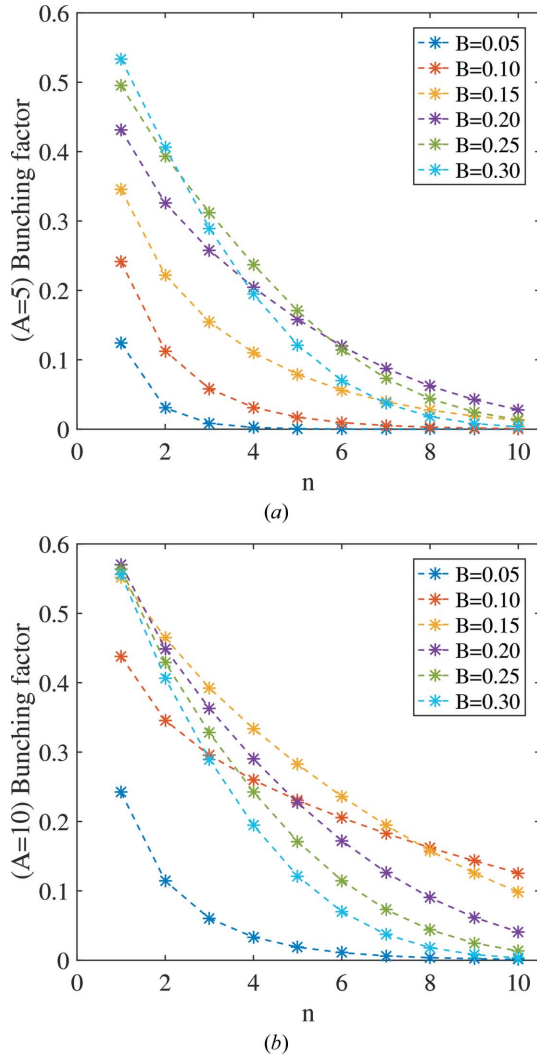
Figure 3
Bunching factor versus harmonic number for the case of (a) A = 5 and (b) A = 10. The curves correspond to the cases of the different dispersion strengths.

Table 2
Main parameters of the seed laser and undulators.

Parameter	Symbol	Value	Unit
Seed laser parameter			
Wavelength	λ_l	266	nm
Power	P_l	0.5–2	TW
Rayleigh length	Z_R	0.8	m
Pulse duration (FWHM)	τ_l	8	fs
Modulator undulator			
Length	L_m	0.3	m
Period length	$\lambda_{m,u}$	6	cm
Undulator parameter	K_m	3.054	–
Radiator undulator			
Length	L_r	0.6	m
Period length	$\lambda_{r,u}$	3.4	cm
Undulator parameter	K_r	0.5–4.3	–

smear out the microbunching due to the large energy modulation, which makes it impossible for further FEL gain after the CHG process. Consequently, a short radiator of less than 0.6 m is long enough for the proposed scheme. From the discussions above, the total length of the whole CHG scheme including a triplet, a modulator and a radiator is shorter than 2 m.

3. Beam tracking and FEL simulations

In order to demonstrate the possible performance of the proposed scheme, numerical start-to-end simulations are necessary, presenting various aspects of the beam phase space and the FEL process. The main parameters of the LPA facility at Shanghai Institute of Optics and Fine Mechanics have been shown in Table 1 (Liu *et al.*, 2017); the parameters of the seed laser and the planar undulators are listed in Table 2. Particle generation and tracking through the beamline are performed using the tracking code *Elegant* (Borland, 2000). After the beam optics, the electron beam passing into the following modulator and the next radiator is simulated using the code *Genesis* (Reiche, 1999).

The evolution of the beam longitudinal phase space at the exit of the modulator is presented in Fig. 4. Both energy modulation and density modulation occur in this segment, and most of the particles are concentrated in the narrow spikes around the zero phase of the seed laser. It is noted that the relative energies of the modulated electrons are distributed in a broad range from 750 to 850, such that the scheme is feasible for the operation of the CHG mode instead of the high-gain harmonic generation (HGHG) mode.

To illustrate such an expected radiation generation, we firstly take into account third-harmonic radiation, *i.e.* generating an 88 nm radiation pulse, which is presented in Fig. 5. For comparison purposes, the simulation results for the self-amplified spontaneous emission (SASE) (Kondratenko & Saldin, 1980; Bonifacio *et al.*, 1984) case are also obtained, which present the results of the spontaneous radiation without FEL gain due to the large energy spread of the electron beam. Fig. 5(a) shows the simulated FEL peak power growth along
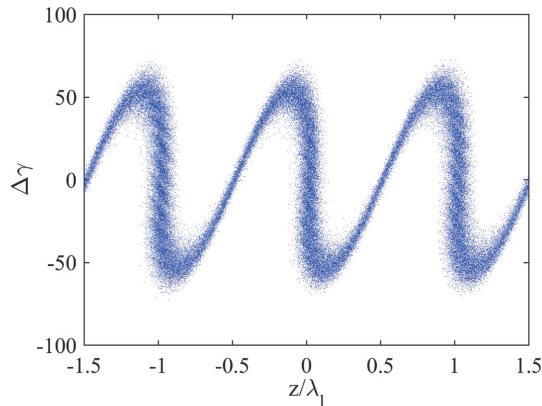
for the FEL generation. The CHG process usually occurs within the first two FEL gain lengths (Yu, 1991). Due to the large initial energy spread, the exponential gain is difficult to attain, such that the required radiator length is only about several times the gain length. We insert the optimized electron beam, laser and undulator parameters into the Pierce parameter equation (Huang & Kim, 2007)

$$\rho_0 = \left[\frac{1}{8\pi} \frac{I_p}{I_A} \left(\frac{K_r[JJ]}{1 + K_r^2/2} \right)^2 \frac{\gamma \lambda_r^2}{\Sigma_A} \right]^{1/3}, \qquad (4)$$

where $K_r[JJ]$ is the undulator parameter of the radiator, and λ_r is the corresponding radiation wavelength. Let us assume that the harmonic number $n = 3$, the average beam size $\sigma_{x,y} = 50\ \mu m$ and the undulator period length $\lambda_u = 3.4$ cm. The main one-dimensional FEL parameters can be estimated as: $\rho_0 \simeq 0.01$, $L_{g0} \simeq 0.15$ m and, while 1% slice energy spread is included, the modified gain length is $L_g \simeq 0.3$ m (Xie, 2000). For the proposed scheme, the radiator dispersion will quickly

Figure 4
Longitudinal phase space of the LPA beam at the exit of the modulator.

the undulator. It can be clearly seen that after a radiator length of 0.6 m the output peak power of the CHG case is up to around 4 GW, which is over five orders of magnitude higher than for synchrotron radiation. According to equation (1), the CHG power growth is quadratically proportional to the undulator length. The simulated result is essentially in agreement with this relation within the first 0.2 m distance. While the microbunching is smeared out rapidly due to the large energy modulation and the radiator dispersion, as a

consequence the peak power is saturated after a distance of about 0.4 m. The output FEL spectra are presented in Fig. 5(b). Manipulated by the seed laser in γ–z space, the CHG radiation is fully coherent with a single and relatively narrow spike structure. And the bandwidth is about 1.5%, which is very close to the Fourier transform-limited bandwidth considering the radiation pulse with pulse length of about 0.7 μm and wavelength of 88 nm. As we know, the regular SASE mode requires quite a long undulator to obtain an exponential gain. However, the radiation pulse will quickly slip out of the electron beam in our simulation due to the relative long radiation wavelength. As a result, the exponential gain will never appear for the synchrotron radiation case and the output radiation power will be very low even for a longer undulator. The CHG peak power with respect to the beam longitudinal position s and the coherent transverse pattern is presented in Figs. 5(c) and 5(d), respectively.

In addition, due to a relatively large energy modulation ($A \simeq 5$), higher harmonics can also be generated. Looking back to Fig. 3, we note that the maximal bunching factor of the seventh harmonic can still be larger than 0.1. The 38 nm radiation, the seventh harmonic of the 266 nm seed laser, is simulated here and is shown in Fig. 6. The results show that 38 nm radiation with an output peak power of >60 MW and a ~1% bandwidth spike is achievable.
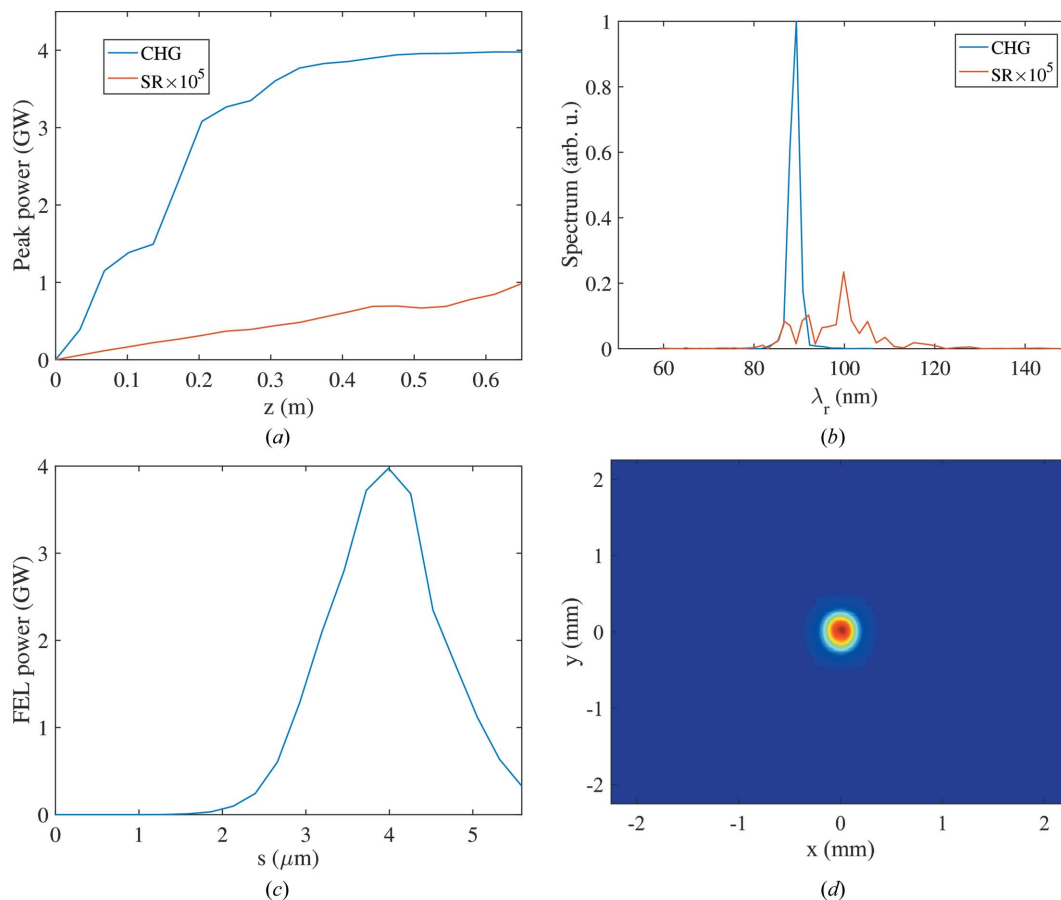

Figure 5
(a) Third-harmonic FEL peak power growth for the CHG case (blue) and the synchrotron radiation case (red). (b) Radiation spectra for the CHG case (blue) and the synchrotron radiation case (red). (c) CHG peak power versus beam longitudinal position. (d) CHG radiation transverse pattern.
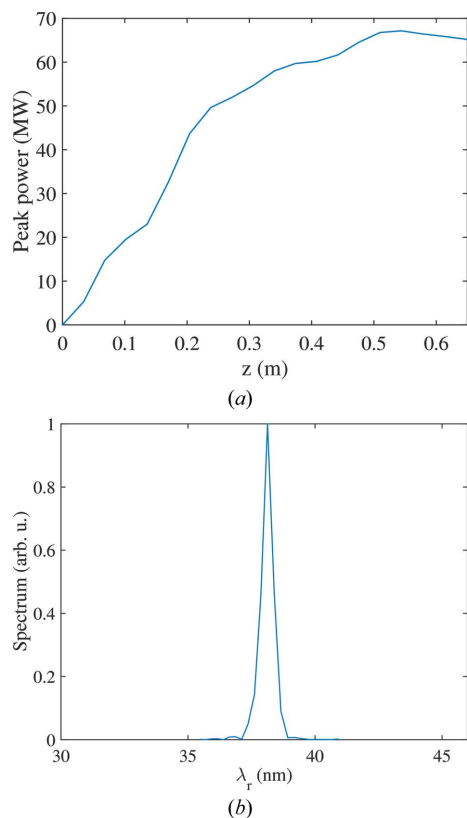
Figure 6
Seventh-harmonic radiation for the proposed CHG case.

4. Practical issues

The performance of the proposed CHG scheme will be affected by some practical issues, such as beam quality degradation and six-dimensional distribution jitter. The LPA beam is generated and accelerated within the centimetres scale, such that it is almost determined by the shot-to-shot ultrahigh-power laser and the ultradense plasma gas. Currently, the LPA technology is still in development, which limits the electron beam quality to be comparable with that of an RF-based linac.

The beam quality fluctuations mainly include peak current, transverse emittance and energy spread. Fig. 7 shows the simulation results of the output power with the variations of these three factors. According to equation (1), the CHG peak power is proportional to the square of the peak current, the reciprocal of the transverse area, and nearly independent of energy spread. Fig. 7(a) presents a quadratic power growth with the increase of bunch charge (i.e. peak current), which appears to correspond to a high degree with the theory. A radiation pulse with a power of 250 MW is still achievable when the charge is reduced to 20 pC. However, the curves in Figs. 7(b) and 7(c) show some disagreement with the theoretical expression, the common reason being that these two factors would affect the beam optics upstream. From the results, a beam with a relatively large emittance of 0.88 mm mrad can still generate a radiation pulse with a power of 550 MW, since the seed laser spot size is large enough to
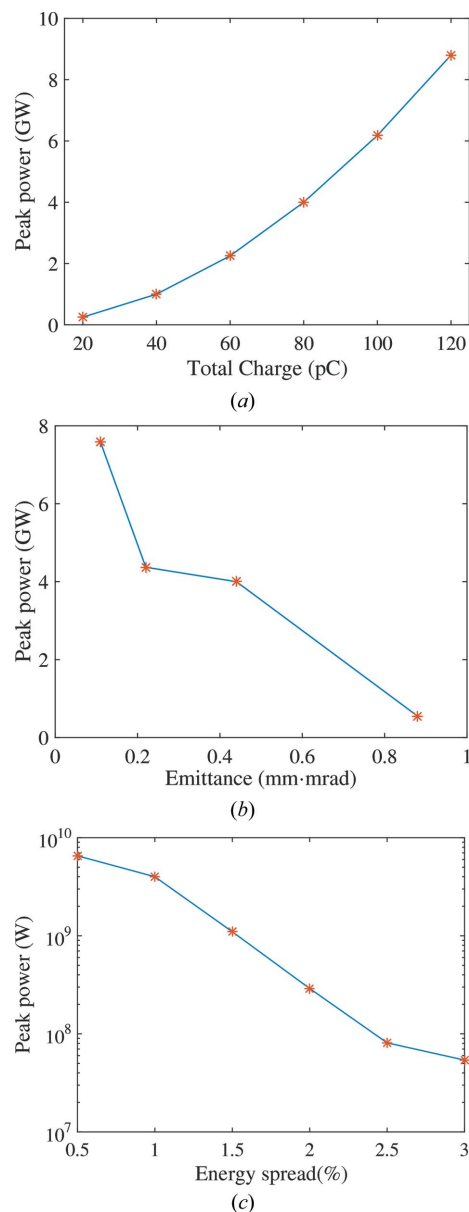

Figure 7
Peak power versus beam quality parameters including total charge, transverse emittance and energy spread.

overlap such an electron beam and induce a deep energy modulation. For the energy spread, the energy modulation amplitude $A = \Delta\gamma/\sigma_\gamma$ indicates that the amplitude A is inversely proportional to the initial energy spread, impacting on the bunching factor of the nth harmonic. Even so, a radiation pulse with a peak power of ~ 50 MW is also attainable when the energy spread is increased to 3% in this scheme.

The six-dimensional distribution jitter usually includes transverse position jitter, incidence angle jitter and central energy jitter. Firstly, let us consider the central energy jitter. Here, energy jitter mainly affects the beam optics and bunching factor. The electrons suffer energy-dependent focusing, such that the average beam sizes in the undulators will be mismatched and degrade the FEL gain. Fig. 8(a) shows the output peak power with respect to energy deviation,

showing that about 10% energy jitter is tolerable and can still generate a radiation power larger than 10 MW. Next, we consider the transverse angle jitter and position jitter that will affect the central trajectory of the electron beam. The orbit change leads to degradations of beam transport and an overlap with the seed laser. For the proposed scheme, the triplet enables the orbit deviation to be corrected to some degree. As shown in Fig. 8(b), an 800 µrad incidence angle jitter degrades the FEL peak power by less than one order of

magnitude. Fig. 8(c) presents the output peak power with different position deviation; the blue curve shows that a 100 µm position jitter can generate a peak power of >10 MW. When one increases the Rayleigh length of the seed laser to 5 m (red curve), the output peak power over 10 MW can be generated in the range of 200 µm position jitter, despite a certain power degradation for the reference beam without position deviation.

It is worth noting that for our CHG scheme we assume an LPA beam with a slice energy spread that is 1% free of energy chirp. Actually, both LPA theory and experiment indicate the existence of energy chirp, but the ultrashort bunch length hinders the direct measurement of the energy chirp and the slice energy spread experimentally (Lin *et al.*, 2012; Maier *et al.*, 2012; Wu *et al.*, 2017). For a chirped electron beam with a smaller slice energy spread, the FEL gain length can be small and the bunching factor can be significantly enhanced, as a result of which it is possible to generate FEL gain and much shorter wavelength radiation for the proposed scheme.

5. Summary

In this paper, we have proposed a simple LPA-based CHG method to achieve significant ultrashort and fully coherent radiation. Both theoretical analysis and numerical simulations were performed to demonstrate the validity of the scheme. This proposed scheme, including a quadrupole triplet, two short undulators and a seed laser, enables coherent radiation generation with high peak power via a very compact layout. It generates energy modulation by means of powerful driver laser splitting and converts to a density modulation relying on the dispersion of the modulator itself. Although lacking exponential gain, intense radiation up to several gigawatts can be produced for the third harmonic of the 266 nm laser, and even the seventh harmonic is also achievable at the 10 MW level. It is worth mentioning that this scheme has a great tolerance to the LPA beam with an instable beam quality and considerable phase space jitter. It has great potential to achieve FEL gain and much shorter wavelength radiation with a smaller slice energy spread. Consequently, the special CHG scheme enables realization of an LPA-based FEL and provides a possible way to the development of the compact FEL.
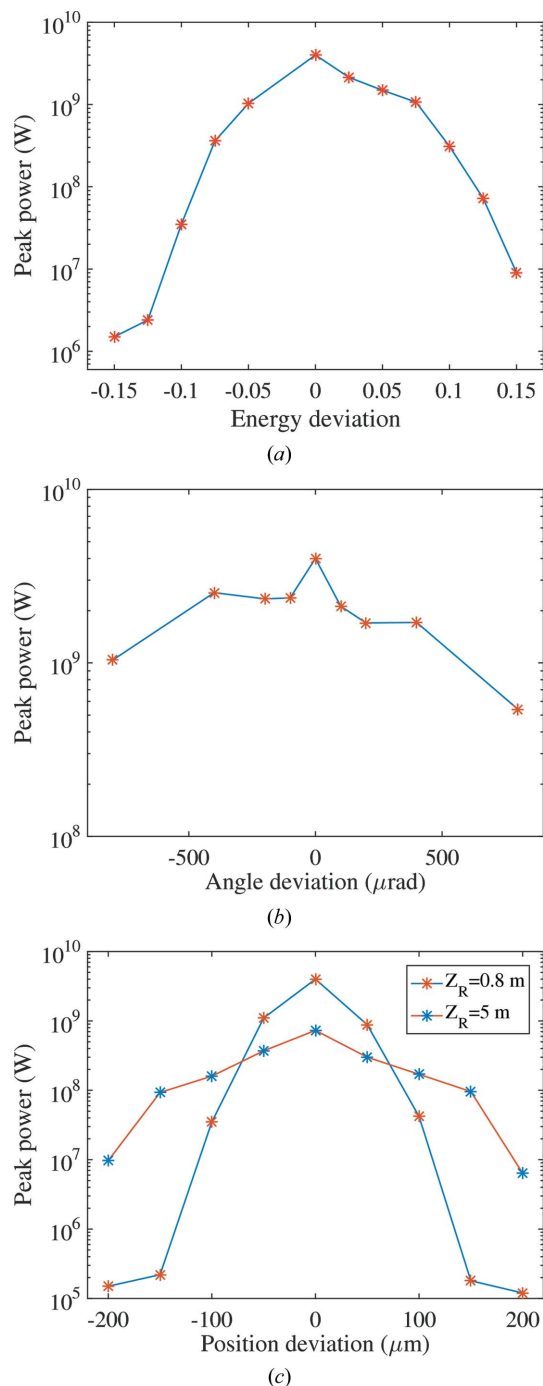
Figure 8
Peak power versus six-dimensional phase space jitters including energy jitter, incident angle jitter and position jitter.

References

Ackermann, W., Asova, G., Ayvazyan, V., Azima, A., Baboi, N., Bähr, J., Balandin, V., Beutner, B., Brandt, A., Bolzmann, A., Brinkmann, R., Brovko, O. I., Castellano, M., Castro, P., Catani, L., Chiadroni, E., Choroba, S., Cianchi, A., Costello, J. T., Cubaynes, D., Dardis, J., Decking, W., Delsim-Hashemi, H., Delserieys, A., Di Pirro, G., Dohlus, M., Düsterer, S., Eckhardt, A., Edwards, H. T., Faatz, B., Feldhaus, J., Flöttmann, K., Frisch, J., Fröhlich, L., Garvey, T., Gensch, U., Gerth, Ch., Görler, M., Golubeva, N., Grabosch, H.-J., Grecki, M., Grimm, O., Hacker, K., Hahn, U., Han, J. H., Honkavaara, K., Hott, T., Hüning, M., Ivanisenko, Y., Jaeschke, E., Jalmuzna, W., Jezynski, T., Kammering, R., Katalev, V., Kavanagh, K., Kennedy, E. T., Khodyachykh, S., Klose, K., Kocharyan, V., Körfer, M., Kollewe, M., Koprek, W., Korepanov, S., Kostin, D., Krassilnikov, M., Kube, G., Kuhlmann, M., Lewis, C. L. S., Lilje, L., Limberg, T., Lipka, D., Löhl, F., Luna, H., Luong, M., Martins, M., Meyer, M., Michelato, P., Miltchev, V., Möller, W. D., Monaco, L., Müller, W. F. O., Napieralski, O., Napoly, O., Nicolosi, P., Nölle, D., Nuñez, T., Oppelt, A., Pagani, C., Paparella, R., Pchalek, N., Pedregosa-Gutierrez, J., Petersen, B., Petrosyan, B., Petrosyan, G., Petrosyan, L., Pflüger, J., Plönjes, E., Poletto, L., Pozniak, K., Prat, E., Proch, D., Pucyk, P., Radcliffe, P., Redlin, H., Rehlich, K., Richter, M., Roehrs, M., Roensch, J., Romaniuk, R., Ross, M., Rossbach, J., Rybnikov, V., Sachwitz, M., Saldin, E. L., Sandner, W., Schlarb, H., Schmidt, B., Schmitz, M., Schmüser, P., Schneider, J. R., Schneidmiller, E. A., Schnepp, S., Schreiber, S., Seidel, M., Sertore, D., Shabunov, A. V., Simon, C., Simrock, S., Sombrowski, E., Sorokin, A. A., Spanknebel, P., Spesyvtsev, R., Staykov, L., Steffen, B., Stephan, F., Stulle, F., Thom, H., Tiedtke, K., Tischer, M., Toleikis, S., Treusch, R., Trines, D., Tsakov, I., Vogel, E., Weiland, T., Weise, H., Wellhöfer, M., Wendt, M., Will, I., Winter, A., Wittenburg, K., Wurth, W., Yeates, P., Yurkov, M. V., Zagorodnov, I. & Zapfe, K. (2007). *Nat. Photon.* **1**, 336–342.

Allaria, E., Appio, R., Badano, L., Barletta, W. A., Bassanese, S., Biedron, S. G., Borga, A., Busetto, E., Castronovo, D., Cinquegrana, P., Cleva, S., Cocco, D., Cornacchia, M., Craievich, P., Cudin, I., D'Auria, G., Dal Forno, M., Danailov, M. B., De Monte, R., De Ninno, G., Delgiusto, P., Demidovich, A., Di Mitri, S., Diviacco, B., Fabris, A., Fabris, R., Fawley, W., Ferianis, M., Ferrari, E., Ferry, S., Froehlich, L., Furlan, P., Gaio, G., Gelmetti, F., Giannessi, L., Giannini, M., Gobessi, R., Ivanov, R., Karantzoulis, E., Lonza, M., Lutman, A., Mahieu, B., Milloch, M., Milton, S. V., Musardo, M., Nikolov, I., Noe, S., Parmigiani, F., Penco, G., Petronio, M., Pivetta, L., Predonzani, M., Rossi, F., Rumiz, L., Salom, A., Scafuri, C., Serpico, C., Sigalotti, P., Spampinati, S., Spezzani, C., Svandrlik, M., Svetina, C., Tazzari, S., Trovo, M., Umer, R., Vascotto, A., Veronese, M., Visintini, R., Zaccaria, M., Zangrando, D. & Zangrando, M. (2012). *Nat. Photon.* **6**, 699–704.

Bonifacio, R., Pellegrini, C. & Narducci, L. (1984). *Opt. Commun.* **50**, 373–378.

Borland, M. (2000). *elegant: A Flexible SDDS-Compliant Code for Accelerator Simulation*, Presented at the *6th International Computational Accelerator Physics Conference (ICAP2000)*, 11–14 September 2000, Darmstadt, Germany. Report No. LS-287.

Bostedt, C., Boutet, S., Fritz, D. M., Huang, Z., Lee, H. J., Lemke, H. T., Robert, A., Schlotter, W. F., Turner, J. J. & Williams, G. J. (2016). *Rev. Mod. Phys.* **88**, 015007.

Chapman, H. N., Fromme, P., Barty, A., White, T. A., Kirian, R. A., Aquila, A., Hunter, M. S., Schulz, J., DePonte, D. P., Weierstall, U., Doak, R. B., Maia, F. R. N. C., Martin, A. V., Schlichting, I., Lomb, L., Coppola, N., Shoeman, R. L., Epp, S. W., Hartmann, R., Rolles, D., Rudenko, A., Foucar, L., Kimmel, N., Weidenspointner, G., Holl, P., Liang, M., Barthelmess, M., Caleman, C., Boutet, S., Bogan, M. J., Krzywinski, J., Bostedt, C., Bajt, S., Gumprecht, L., Rudek, B., Erk, B., Schmidt, C., Hömke, A., Reich, C., Pietschner, D., Strüder, L., Hauser, G., Gorke, H., Ullrich, J., Herrmann, S., Schaller, G., Schopper, F., Soltau, H., Kühnel, K., Messerschmidt, M., Bozek, J. D., Hau-Riege, S. P., Frank, M., Hampton, C. Y., Sierra, R. G., Starodub, D., Williams, G. J., Hajdu, J., Timneanu, N., Seibert, M. M., Andreasson, J., Rocker, A., Jönsson, O., Svenda, M., Stern, S., Nass, K., Andritschke, R., Schröter, C., Krasniqi, F., Bott, M., Schmidt, K. E., Wang, X., Grotjohann, I., Holton, J. M., Barends, T. R. M., Neutze, R., Marchesini, S., Fromme, R., Schorb, S., Rupp, D., Adolph, M., Gorkhover, T., Andersson, I., Hirsemann, H., Potdevin, G., Graafsma, H., Nilsson, B. & Spence, J. C. H. (2011). *Nature*, **470**, 73–77.

De Ninno, G., Allaria, E., Coreno, M., Curbis, F., Danailov, M. B., Karantzoulis, E., Locatelli, A., Menteş, T. O., Nino, M. A., Spezzani, C. & Trovò, M. (2008). *Phys. Rev. Lett.* **101**, 053902.

Emma, P., Akre, R., Arthur, J., Bionta, R., Bostedt, C., Bozek, J., Brachmann, A., Bucksbaum, P., Coffee, R., Decker, F. J., Ding, Y., Dowell, D., Edstrom, S., Fisher, A., Frisch, J., Gilevich, S., Hastings, J., Hays, G., Hering, P., Huang, Z., Iverson, R., Loos, H., Messerschmidt, M., Miahnahri, A., Moeller, S., Nuhn, H. D., Pile, G., Ratner, D., Rzepiela, J., Schultz, D., Smith, T., Stefan, P., Tompkins, H., Turner, J., Welch, J., White, W., Wu, J., Yocky, G. & Galayda, J. (2010). *Nat. Photon.* **4**, 641–647.

Esarey, E., Schroeder, C. B. & Leemans, W. P. (2009). *Rev. Mod. Phys.* **81**, 1229–1285.

Feng, C., Xiang, D., Deng, H., Huang, D., Wang, D. & Zhao, Z. (2015). *Opt. Express*, **23**, 14993–15002.

Fuchs, M., Weingartner, R., Popp, A., Major, Z., Becker, S., Osterhoff, J., Cortrie, I., Zeitler, B., Hörlein, R., Tsakiris, G. D., Schramm, U., Rowlands-Rees, T. P., Hooker, S. M., Habs, D., Krausz, F., Karsch, S. & Grüner, F. (2009). *Nat. Phys.* **5**, 826–829.

Ghaith, A., Marteau, F., N'gotta, P., Kitegi, C., Andre, T., Valleau, M., Veteran, J., Blache, F., Benabderrahmane, C., Cosson, O., Forest, F., Jivkov, P., Lancelot, J. L. & Couprie, M. E. (2017). *Proceedings of the 38th International Free-Electron Laser Conference (FEL2017)*, 20–25 August 2017, Santa Fe, NM, USA, pp. 542–545. WEP064.

Girard, B., Lapierre, Y., Ortega, J. M., Bazin, C., Billardon, M., Elleaume, P., Bergher, M., Velghe, M. & Petroff, Y. (1984). *Phys. Rev. Lett.* **53**, 2405–2408.

Grüner, F., Becker, S., Schramm, U., Eichner, T., Fuchs, M., Weingartner, R., Habs, D., Meyer-ter-Vehn, J., Geissler, M., Ferrario, M., Serafini, L., van der Geer, B., Backe, H., Lauth, W. & Reiche, S. (2007). *Appl. Phys. B*, **86**, 431–435.

Hemsing, E., Stupakov, G., Xiang, D. & Zholents, A. (2014). *Rev. Mod. Phys.* **86**, 897–941.

Huang, Z., Ding, Y. & Schroeder, C. B. (2012). *Phys. Rev. Lett.* **109**, 204801.

Huang, Z. & Kim, K.-J. (2007). *Phys. Rev. ST Accel. Beams*, **10**, 034801.

Ishikawa, T., Aoyagi, H., Asaka, T., Asano, Y., Azumi, N., Bizen, T., Ego, H., Fukami, K., Fukui, T., Furukawa, Y., Goto, S., Hanaki, H., Hara, T., Hasegawa, T., Hatsui, T., Higashiya, A., Hirono, T., Hosoda, N., Ishii, M., Inagaki, T., Inubushi, Y., Itoga, T., Joti, Y., Kago, M., Kameshima, T., Kimura, H., Kirihara, Y., Kiyomichi, A., Kobayashi, T., Kondo, C., Kudo, T., Maesaka, H., Maréchal, X. M., Masuda, T., Matsubara, S., Matsumoto, T., Matsushita, T., Matsui, S., Nagasono, M., Nariyama, N., Ohashi, H., Ohata, T., Ohshima, T., Ono, S., Otake, Y., Saji, C., Sakurai, T., Sato, T., Sawada, K., Seike, T., Shirasawa, K., Sugimoto, T., Suzuki, S., Takahashi, S., Takebe, H., Takeshita, K., Tamasaku, K., Tanaka, H., Tanaka, R., Tanaka, T., Togashi, T., Togawa, K., Tokuhisa, A., Tomizawa, H., Tono, K., Wu, S., Yabashi, M., Yamaga, M., Yamashita, A., Yanagida, K., Zhang, C., Shintake, T., Kitamura, H. & Kumagai, N. (2012). *Nat. Photon.* **6**, 540–544.

Kim, H. T., Pae, K. H., Cha, H. J., Kim, I. J., Yu, T. J., Sung, J. H., Lee, S. K., Jeong, T. M. & Lee, J. (2013). *Phys. Rev. Lett.* **111**, 165002.

Kondratenko, A. M. & Saldin, E. L. (1980). *Part. Accel.* **10**, 207–216.

Labat, M., Hosaka, M., Mochihashi, A., Shimada, M., Katoh, M., Lambert, G., Hara, T., Takashima, Y. & Couprie, M. E. (2007). *Eur. Phys. J. D*, **44**, 187–200.

Leemans, W. P., Gonsalves, A. J., Mao, H.-S., Nakamura, K., Benedetti, C., Schroeder, C. B., Tóth, C., Daniels, J., Mittelberger, D. E., Bulanov, S. S., Vay, J.-L., Geddes, C. G. R. & Esarey, E. (2014). *Phys. Rev. Lett.* **113**, 245002.

Li, W.-T., Wang, W.-T., Liu, J.-S., Wang, C., Zhang, Z.-J., Qi, R., Yu, C.-H., Li, R.-X. & Xu, Z.-Z. (2015). *Chin. Phys. B*, **24**, 015205.

Lin, C., van Tilborg, J., Nakamura, K., Gonsalves, A. J., Matlis, N. H., Sokollik, T., Shiraishi, S., Osterhoff, J., Benedetti, C., Schroeder, C. B., Tóth, C., Esarey, E. & Leemans, W. P. (2012). *Phys. Rev. Lett.* **108**, 094801.

Liu, J. S., Xia, C. Q., Wang, W. T., Lu, H. Y., Wang, C., Deng, A. H., Li, W. T., Zhang, H., Liang, X. Y., Leng, Y. X., Lu, X. M., Wang, C., Wang, J. Z., Nakajima, K., Li, R. X. & Xu, Z. Z. (2011). *Phys. Rev. Lett.* **107**, 035001.

Liu, T., Liu, B. D., Wang, Zhang, T., Huang, Z. & Liu, J. S. (2016). *Proceedings of the 7th International Particle Accelerator Conference (IPAC2016)*, 8–13 May 2016, Busan, Korea, pp. 3287–3290. THPMB027.

Liu, T., Zhang, T., Wang, D. & Huang, Z. (2017). *Phys. Rev. Accel. Beams*, **20**, 020701.

Loulergue, A., Labat, M., Evain, C., Benabderrahmane, C., Malka, V. & Couprie, M. E. (2015). *New J. Phys.* **17**, 023028.

Maier, A. R., Meseck, A., Reiche, S., Schroeder, C. B., Seggebrock, T. & Grüner, F. (2012). *Phys. Rev. X*, **2**, 031019.

Nakajima, K. (2008). *Nat. Phys.* **4**, 92–93.

Reiche, S. (1999). *Nucl. Instrum. Methods Phys. Res. A*, **429**, 243–248.

Schroeder, C. B., Esarey, E., Leemans, W. P., van Tilborg, J., Grüner, F. F., Ding, Y., Huang, Z., Grüner, F. J. & Maier, A. R. (2013). *Proceedings of the 35th International Free-Electron Laser Conference (FEL2013)*, 26–30 August 2013, New York, NY, USA, pp. 117–121. MOPSO69.

Schroeder, C. B., Fawley, W. M., Esarey, E. & Leemans, W. P. (2006). *Proceedings of the 28th Internation Free-Electron laser Conference (FEL2006)*, 27 August–1 September 2006, Berlin, Germany, p. 455–458. TUPPH055.

Tajima, T. & Dawson, J. M. (1979). *Phys. Rev. Lett.* **43**, 267–270.

Wang, W. T., Li, W. T., Liu, J. S., Zhang, Z. J., Qi, R., Yu, C. H., Liu, J. Q., Fang, M., Qin, Z. Y., Wang, C., Xu, Y., Wu, F. X., Leng, Y. X., Li, R. X. & Xu, Z. Z. (2016). *Phys. Rev. Lett.* **117**, 124801.

Wang, X., Zgadzaj, R., Fazel, N., Li, Z., Yi, S. A., Zhang, X., Henderson, W., Chang, Y. Y., Korzekwa, R., Tsai, H. E., Pai, C. H., Quevedo, H., Dyer, G., Gaul, E., Martinez, M., Bernstein, A. C., Borger, T., Spinks, M., Donovan, M., Khudik, V., Shvets, G., Ditmire, T. & Downer, M. C. (2013). *Nat. Commun.* **4**, 1988.

Widmann, C., Rodriguez, V. A., Bernhard, A., Braun, N., Härer, B., Jäckel, O., Nicolai, M., Peiffer, P., Reuter, M., Rinck, T., Rossmanith, R., Sävert, A., Scheer, M., Werner, W., Baumbach, T. & Kaluza, M. C. (2013). *Proceedings of the 4th International Particle Accelerator Conference (IPAC2013)*, 15–20 June 2014, Shanghai, China, pp. 60–63. TUPWO013.

Widmann, C., Rodriguez, V. A. & Braun, N. (2014). *Proceedings of the 5th International Particle Accelerator Conference (IPAC2014)*, 15–20 June 2014, Dresden, Germany, pp. 2803–2806. THOBA03.

Wu, Y., Du, Y., Zhang, J., Zhou, Z., Cheng, Z., Zhou, S., Hua, J., Pai, C. & Lu, W. (2017). *Proceedings of the 8th International Particle Accelerator Conference (IPAC2017)*, 14–19 May 2017, Copenhagen, Denmark, pp. 1258–1260. TUOBB1.

Xiang, D. & Wan, W. (2010). *Phys. Rev. Lett.* **104**, 084803.

Xie, M. (2000). *Nucl. Instrum. Methods Phys. Res. A*, **445**, 59–66.

Young, L., Kanter, E. P., Krssig, B., Li, Y., March, A. M., Pratt, S. T., Santra, R., Southworth, S. H., Rohringer, N., DiMauro, L. F., Doumy, G., Roedig, C. A., Berrah, N., Fang, L., Hoener, M., Bucksbaum, P. H., Cryan, J. P., Ghimire, S., Glownia, J. M., Reis, D. A., Bozek, J. D., Bostedt, C. & Messerschmidt, M. (2010). *Nature*, **466**, 56–61.

Yu, L.-H. (1991). *Phys. Rev. A*, **44**, 5178–5193.

Yu, L.-H., Babzien, M., Ben-Zvi, I., DiMauro, L. F., Doyuran, A., Graves, W., Johnson, E., Krinsky, S., Malone, R., Pogorelsky, I., Skaritka, J., Rakowsky, G., Solomon, L., Wang, X. J., Woodle, M., Yakimenko, V., Biedron, S. G., Galayda, J. N., Gluskin, E., Jagger, J., Sajaev, V. & Vasserman, I. (2000). *Science*, **289**, 932–934.